On the singular, dual, and multiple positional specificity of manganese lipoxygenase and its G316A mutant

Mirela Cristea and Ernst H. Oliw[1]

Division of Biochemical Pharmacology, Department of Pharmaceutical Biosciences, Uppsala University Biomedical Center, SE-751 24 Uppsala, Sweden

Abstract **Abstract manganese lipoxygenase (Mn-LO) oxygenates 18:3n-3 and 18:2n-6 to *bis*-allylic 11*S*-hydroperoxy fatty acids, which are converted to 13*R*-hydroperoxy fatty acids. Other unsaturated C_{16}-C_{22} fatty acids, except 17:3n-3, are poor substrates, possibly because of ineffective enzyme activation ($Mn^{II} \rightarrow Mn^{III}$) by the produced hydroperoxides. Our aim was to determine whether unsaturated C_{16}-C_{22} fatty acids were oxidized by Mn^{III}-LO. Mn^{III}-LO oxidized C_{16}, C_{19}, C_{20}, and C_{22} n-3 and n-6 fatty acids. The carbon chain length influenced the position of hydrogen abstraction (n-8, n-5) and oxygen insertion at the terminal or the penultimate 1*Z*,4*Z*-pentadienes. Dilinoleoyl-glycerophosphatidylcholine was oxidized by Mn-LO, in agreement with a "tail-first" model. 16:3n-3 was oxidized at the *bis*-allylic n-5 carbon and at positions n-3, n-7, and n-6. Long fatty acids, 19:3n-3, 20:3n-3, 20:4n-6, 22:5n-3, and 22:5n-6, were oxidized mainly at the n-6 and the *bis*-allylic n-8 positions (in ratios of ~3:2). The *bis*-allylic hydroperoxides accumulated with one exception, 13-hydroperoxyeicosatetraenoic acid (13-HPETE). Mn^{III}-LO oxidized 20:4n-6 to 15*R*-HPETE (~60%) and 13-HPETE (~37%) and converted 13-HPETE to 15*R*-HPETE. Mn^{III}-LO G316A oxygenated mainly 16:3n-3 at positions n-7 and n-6, 19:3n-3 at n-10, n-8, and n-6, and 20:3n-3 at n-10 and n-8. We conclude that Mn-LO likely binds fatty acids tail-first and oxygenates many C_{16}, C_{18}, C_{20}, and C_{22} fatty acids to significant amounts of *bis*-allylic hydroperoxides.—**Cristea, M., and E. H. Oliw. **On the singular, dual, and multiple positional specificity of manganese lipoxygenase and its G316A mutant. *J. Lipid Res.* 2007.** 48: **890–903.**

Supplementary key words nonconjugated peroxyls • fatty acid oxygenation • hydroperoxide isomerase • mass spectrometry • metalloenzymes • dilinoleoyl-glycerophosphatidylcholine • thermostability

Lipoxygenases are Fe- or Mn-containing dioxygenases of polyunsaturated fatty acids (1) [the LOX-DB at www.dkfz-heidelberg.de/spec/lox-db/, as described (1a)]. Fe-lipoxygenases are widely spread in plants and animals (2–4), whereas manganese lipoxygenase (Mn-LO) occurs in *Gaeumannomyces graminis*, a root pathogen of wheat (5). All lipoxygenases belong to the same gene family (1, 4, 6, 7). The three-dimensional structures are available for lipoxygenases from soybean, rabbit reticulocytes, and coral (8–13). Lipoxygenation occurs by hydrogen abstraction at the methylene carbon of the 1*Z*,4*Z*-pentadiene followed by O_2 insertion with the formation of hydroperoxy fatty acids (1, 3, 4). The hydroperoxides are precursors of signal molecules in plants and animals and may take part in the chemical warfare between plants, fungi, and other microorganisms (1–3, 14). Lipoxygenases may also oxidize esterified polyunsaturated fatty acids of lipid membranes (15).

Mn-LO is a glycosylated protein of 90–100 kDa that is secreted by *G. graminis* (5). Mn-LO differs from all lipoxygenases in two respects. It catalyzes the oxygenation of 18:2n-6 by suprafacial hydrogen ($H^{\bullet}$ atom) abstraction at C-11 and by O_2 insertion at the *bis*-allylic position C-11 and at C-13 with the formation of 11*S*-hydroperoxyoctadecadienoic acid (11*S*-HPODE) and 13*R*-HPODE in a 1:4 ratio (16). 11*S*-HPODE is transformed to 13*R*-HPODE by Mn-LO (16). 18:3n-3 is oxidized in analogy with 18:2n-6, whereas 17:3n-3 is converted mainly to the n-6 hydroperoxy fatty acid (17). In addition, Mn-LO also transforms 13*R*-hydroperoxyoctadecatrienoic acid (13*R*-HPOTrE) to 13-ketooctadecatrienoic acid and to epoxyalcohols (17). The prototype Fe-lipoxygenase, soybean lipoxygenase-1 (sLO-1), catalyzes antarafacial hydrogen abstraction and O_2 insertion at C-13 [or at C-9 in a pH-dependent manner (1, 18)]. The spin density of the carbon-centered 1*Z*,4*Z*-pentadiene ψ is highest at C-3 (19), yet hydroperoxides at this *bis*-allylic position are not formed to a significant extent by naturally occurring Fe-lipoxygenases (20–22). To date, significant oxygenation of *bis*-allylic carbons by Fe-

Manuscript received 28 November 2006 and in revised form 16 January 2007 and in re-revised form 26 January 2007.

Published, JLR Papers in Press, January 26, 2007.
DOI 10.1194/jlr.M600505-JLR200

Abbreviations: CP, chiral phase; GPC, glycerophosphatidylcholine; HETE, hydroxyeicosatetraenoic acid; HHTrE, hydroxyhexadecatrienoic acid; HNTrE, hydroxynonadecatrienoic acid; HPETE, hydroperoxyeicosatetraenoic acid; HPHTrE, hydroperoxyhexadecatrienoic acid; HPNTrE, hydroperoxynonadecatrienoic acid; HPODE, hydroperoxyoctadecadienoic acid; HPOTrE, hydroperoxyoctadecatrienoic acid; KETE, ketoeicosatetraenoic acid; KETrE, ketoeicosatrienoic acid; KHTrE, ketohexadecatrienoic acid; KNTrE, ketononadecatrienoic acid; LOX, lipoxygenase; Mn-LO, manganese lipoxygenase; NP, normal-phase; RP, reverse-phase; sLO, soybean lipoxygenase; TPP, triphenylphosphine; UV, ultraviolet.

[1] To whom correspondence should be addressed.
e-mail: ernst.oliw@farmbio.uu.se

lipoxygenases has only been reported for the recombinant lipoxygenase domain of allene oxide synthase of *Plexaura homomalla*, which transforms 20:3n-6 to the *bis*-allylic hydroperoxide at C-10 (~5%) and to the conjugated hydroperoxide with *R* configuration at C-8 (~95%) (23). For comparison, rice leaf pathogen-inducible Fe-lipoxygenase generates 0.4% 11-HPODE besides the main product, 13*S*-HPODE (20).

The lipoxygenation of fatty acids starts slowly with a characteristic time lag until the enzyme is fully oxidized to its active forms, Fe^{III}-LO and Mn^{III}-LO (20, 24–26). Oxidation then proceeds at a linear rate and ends with consumption of the substrate, yielding a characteristic kinetic trace. Key factors triggering lipoxygenation are the produced hydroperoxides (24, 25, 27). The lipoxygenase may contain a small fraction of activated enzyme. This fraction will oxidize the substrate to hydroperoxides, which in turn will activate the enzyme in a chain reaction. It is also conceivable that hydroperoxides present in the substrates may start this reaction. Fatty acid hydroperoxides may differ in their capacity to activate lipoxygenases (27). Mn-LO is readily activated by 13*R*-hydroperoxides of 18:2n-6, 18:3n-3, and 17:3n-3, but whether hydroperoxides of shorter or longer fatty acids also activate Mn-LO is unknown.

The oxidation of C_{16}-C_{22} free fatty acids and dilinoleoyl-glycerophosphatidylcholine (GPC) by Mn-LO may provide information on five related processes: *i*) fatty acid binding to the active site so that *bis*-allylic carbons can be subjected to hydrogen abstraction; *ii*) the orientation of the fatty acid at the active site; *iii*) O_2 insertion at the 1, 3, or 5 position of the carbon-centered pentadiene radical; *iv*) enzyme activation by the produced hydroperoxides; and *v*) the mechanism for the transformation of *bis*-allylic hydroperoxides to *cis-trans*-conjugated products (β-fragmentation).

The first four events have been investigated extensively with Fe-lipoxygenases. The effect of *cis* double bonds between the 2,5- and 14,17-positions of 18:2 on the catalytic activity of sLO-1 revealed that the 9,12- and 13,16-isomers were subject to hydrogen abstraction at C-11 and C-15 and to oxygenation at C-13 and C-17, respectively (28, 29). Oxygenation of five regioisomers of 20:4 (n-3 to n-7) could be interpreted in a logical way, as the position of hydrogen abstraction between C-10 and C-13 (sLO-1) and between C-10 and C-14 [15-lipoxygenase (15-LOX)] varied with the positions of the double bonds (4, 30). Site-directed mutagenesis with volume changes at the active site of Fe-lipoxygenases also showed that the positions of hydrogen abstraction and oxygenation of 20:4n-6 could be explained by shifts in alignments of the double bonds with the catalytic metal (3, 4, 31). Lipoxygenases may bind their substrates in two ways, either with the ω-end embedded in the active site ("tail-first"; e.g., 8*R*-LOX, 12*S*-LOX, 15*S*-LOX,) or with the carboxyl group embedded in the protein ("head-first", e.g., 5*S*-LOX, 8*S*-LOX, 12*R*-LOX) (32–34). Lipoxygenases that can oxidize fatty acids in phospholipids belong to the first group (33).

A characteristic feature of *R*-lipoxygenases is a conserved glycine (Gly) residue, whereas *S* lipoxygenases have an alanine (Ala) residue in this position (32, 34). Site-directed mutagenesis of the Gly residue to Ala shifted the oxygenation of the 1*Z*,4*Z*-pentadiene of 12*R*-LOX and 8*R*-LOX from one end to the other. This mutation had little effect on murine 12*R*-LOX with 20:4n-6 and on Mn-LO with 18:3n-3 as substrates (17, 35). The main difference between Mn-LO and its G316A mutant was the augmented hydroperoxide isomerase activity with the formation of epoxyalcohols and keto fatty acids (17).

Our main goal was to determine the orientations of fatty acids in the active site of Mn-LO and to deduce the positions of *bis*-allylic carbons of fatty acids with different chain lengths relative to the catalytic metal. We examined C_{16}-C_{22} n-3 and n-6 fatty acids and dilinoleoyl-GPC and identified the major products. As hydroperoxides might differ in their capacity to oxidize Mn-LO to Mn^{III}-LO, we also evaluated preoxidized enzyme. The second goal was to determine whether Mn^{III}-LO G316A oxygenated a selection of these fatty acids and whether the positional specificity was changed. We also determined whether the catalytic metal of Mn-LO could be extracted and the apoprotein reconstituted in the same way as reported for sLO-3 (36).

EXPERIMENTAL PROCEDURES

Materials

Dilinoleoyl-GPC (99%), 16:3n-3 (99%), 19:3n-3 (99%), 20:3n-3 (99%), 22:5n-6 (99%), 22:5n-3 (99%), and 22:6n-3 (99%) were obtained from Larodan (Malmö, Sweden). 11*S*-Hydroxyeicosatetraenoic acid (11*S*-HETE) and methyl 11*R*,*S*-HETE were from Cayman (Ann Arbor, MI). Methyl esters were hydrolyzed in 0.5 M KOH in methanol with 10% water (1 h, 70°C). [5,6,8,9,11,12,14,15-$^2H_8$]20:4n-6 was a generous gift from the late D. A. van Dorp. 18:2n-6 (99%), 18:3n-6, HPLC solvents (Lichrosolve), and 2,3-dichloro-5,6-dicyanobenzoquinone were from Merck. 20:4n-6 (99%), triphenylphosphine (TPP), and Chelex-100 beads were from Sigma-Aldrich. Fatty acids were dissolved in ethanol and stored in stock solutions (50–100 mM) at −20°C; fresh solutions (50–100 μM) of the fatty acids were prepared in 0.1 M $NaBO_3$ buffer (pH 9.0). 13*R*-HPOTrE was prepared by biosynthesis using Mn-LO, quantified by ultraviolet (UV) absorption, checked by normal-phase (NP)-HPLC with MS/MS detection, and stored in stocks of 6–8 mM in ethanol at −20°C (20). 15*S*-Hydroperoxyeicosatetraenoic acid (15*S*-HPETE), 15*S*-hydroperoxyeicosatrienoic acid (15*S*-HPETrE), 14*S*-hydroperoxynonadecatrienoic acid (14*S*-HPNTrE), and 11*S*-hydroperoxyhexadecatrienoic acid (11*S*-HPHTrE) were prepared by biosynthesis using sLO-1 (Lipoxidase; Sigma), and the hydroperoxides were reduced to alcohols with TPP or $NaBH_4$. Recombinant Mn-LO and Mn-LO G316A were expressed in *Pichia pastoris* (strain X-33) as a secreted protein using the expression vector pPICZAα (7), and the enzymes were purified from the growth medium by hydrophobic interaction and ion-exchange chromatography (7).

Enzyme assay

Light absorbance was measured with a dual-beam spectrophotometer (Shimadzu UV-2101PC). The *cis-trans*-conjugated hydro(pero)xy fatty acids were assumed to have an extinction coefficient of 25,000 cm^{-1} M^{-1} (37). Lipoxygenase activity was monitored by UV spectroscopy (235–237 nm) in 0.1 M $NaBO_3$ buffer (pH 9.0) with 50–100 μM substrate and with 0 or 1–10 μM

13*R*-HPOTrE. The reaction was started by the addition of Mn-LO (10–55 nM). Initially, we preincubated the enzyme with 13*R*-HPOTrE for 1 min and started the reaction by the addition of the substrate, but both procedures yielded the same results. Enzyme activation seemed to be almost instantaneous, and there was no apparent difference between 1 and 10 μM 13*R*-HPOTrE. The cuvettes had to be washed carefully with methanol, water, and buffer between experiments, as traces of hydroperoxides seemed to activate Mn-LO. An aliquot was analyzed at the middle part of the increase in UV absorbance, when the reaction was completed, and 30–60 min thereafter. Products were usually analyzed after extractive isolation [SepPak/C_{18}, as described (7), or extraction with CH_2Cl_2] without acidification. The fatty acid hydroperoxides were reduced to alcohols by treatment with TPP (1–10 μg) before LC-MS/MS analysis. The time lag was estimated as described (27).

HPLC-MS/MS

Reverse-phase (RP)-HPLC-MS/MS was performed with a Surveyor MS pump (Thermo) and an octadecyl silica column (5 μm, 2.1 × 150 mm; Phenomenex), which was usually eluted with methanol-water-acetic acid (750:250:0.06; Suprapur; Merck) at 0.15–0.3 ml/min. The effluent passed a photodiode array detector (Surveyor PDA; 5 cm path length) and was subjected to electrospray ionization in an ion trap mass spectrometer (LTQ; Thermo). The heated transfer capillary was set at 325°C, the ion isolation width at 1.5 amu, and the collision energy at 25 (arbitrary scale). Prostaglandin $F_{1\alpha}$ (100 ng/min) was infused for tuning. The tube lens was usually set to −90 V.

NP-HPLC-MS/MS was performed on silica with an analytical column (Kromasil-100SI; 250 × 2 mm, 5 μm, 100 Å), which was eluted at 0.3–0.5 ml/min with 2, 3, or 5% isopropanol in hexane with 0.05 ml of acetic acid per liter (Constrametric 3200 pump; LDC). This column was regenerated at the end of this study with some loss of resolution (38). The effluent was combined in a tee connectionwith isopropanol-water (3:2; 0.2–0.3 ml/min) from the Surveyor MS pump. The combined effluents were introduced by electrospray into an ion trap mass spectrometer (LTQ). A larger column (Nucleosil 50-5; 250 × 4.6 mm) was used in some experiments and eluted at 1.5 ml/min with 3.5% isopropanol in hexane with 0.1% acetic acid, and separation was monitored by UV detection [photodiode array detector (PDA); Waters 996].

Chiral phase (CP)-HPLC was performed with three columns. Chiralcel OB and Chiralcel OD (25 × 0.46 cm; Daicel through Skandinaviska GeneTech, Kungsbacka, Sweden) were eluted with 3.5% or 5% isopropanol in hexane with 0.1% acetic acid (0.5 ml/min). The effluent was analyzed either by PDA only or by PDA in combination with MS/MS analysis of carboxylate anions, as described for NP-HPLC-MS/MS above. A Pirkle 1A column [25 × 0.46 cm; *R*-(-)*N*-3,5-dinitrobenzoyl-α-phenylglycine ionically bound to the stationary phase; Regis] was used for the steric analysis of 15-HETE methyl ester with UV detection (39).

Thermostability

We followed the method described by Kariapper, Dunham, and Funk (36). The thermostability of Mn-LO (8–15 μg in 50 μl) was assayed in duplicate or triplicate with a PCR instrument (PTC 200; MJ Research) in 0.1 M Tris-HCl (pH 7.0)/0.1 M NaCl and in 0.1 M $NaHCO_3$ (pH 8.0)/0.1 M NaCl (with or without 50 μl of Chelex-100 beads in the same buffer) at temperatures up to 70°C for 30, 60, and 90 min. After cooling, residual lipoxygenase activity was monitored by UV spectroscopy at room temperature with 18:2n-6 as a substrate in 0.1 M $NaBO_3$ (pH 9.0) (7). The manganese content of Mn-LO was determined by inductively coupled plasma atomic emission spectrometry after diafiltration as described (5, 7).

Miscellaneous

Oxidation of *cis-trans*-conjugated hydroxy fatty acids to keto compounds was performed with 2,3-dichloro-5,6-dicyanobenzoquinone as described (40). The keto fatty acids were reduced to racemic hydroxy fatty acids by NaB^2H_4 in methanol on ice (41). Methylation was performed with diazomethane in ether and hydrogenation with Pd/C for 90–120 s (41). 2*S*-Phenylpropionic acid derivatives were prepared and purified as described (41, 42) and analyzed on a capillary GC column (30 m DB-5) coupled to an ion-trap mass spectrometer (Finnigan ITS40) with electron-impact ionization (43). C values were determined from the retention times of saturated fatty acid methyl esters (C_{18}, C_{20}, C_{22}, and C_{24}).

RESULTS

Oxygenation of fatty acids

A series of n-3 and n-6 C_{16}-C_{22} fatty acids was assessed as substrates of both Mn-LO and Mn-LO oxidized to its active form (Mn^{III}-LO) by micromolar concentrations of 13*R*-HPOTrE. The products were first analyzed by RP-HPLC-MS/MS and then by NP-HPLC-MS/MS, which provided better resolution. We also examined whether oxygenation of 16:3n-3, 19:3n-3, 20:3n-3, and 20:4n-6 differed qualitatively between Mn^{III}-LO and its Gly316→Ala mutant.

16:3n-3, 19:3n-3, 20:3n-3, 20:4n-6, 22:5n-3, and 22:5n-6 were oxidized slowly by Mn-LO (15–50 nM) in comparison with 18:3n-3, but the rate increased with 16:3n-3 and 19:3n-3 after a long but distinct kinetic time lag of 3–9 min. In contrast, the oxidized enzyme (Mn^{III}-LO) oxygenated all substrate fatty acids with no time lag. Increasing the enzyme concentration also decreased the lag time (see 20:4n-6 below). The reaction rates were comparatively low with 22:5n-3, 22:5n-6, and dilinoleoyl-GPC. 22:6n-3 and the methyl ester of 18:3n-3 were not oxidized.

16:3n-3. The oxidation of 16:3n-3 by Mn-LO and by Mn-LO in the presence of 13*R*-HPOTrE is shown in **Fig. 1A**. The apparent lag time without 13*R*-HPOTrE was ∼9 min (Fig. 1A), but the time lag was as low as 3 min in some experiments (depending on enzyme concentration). After the lag time, oxidation of 16:3n-3 (∼50 μM) with Mn-LO (55 nM) proceeded at a maximal rate of 0.11 absorbance units per minute [or ∼10% of the oxidation rate of 18:3n-3 (7)]. The time for the conversion of 16:3n-3 to 50% of the totally formed *cis-trans*-conjugated products was reduced by 75% in the presence of 13*R*-HPOTrE. The kinetic trace in the presence of 13*R*-HPOTrE was parabolic and differed from the sigmoid reaction curve of 16:3n-3 with Mn-LO without this activator. The parabolic time curve was noticed in all experiments with 13*R*-HPOTrE as an enzyme activator.

16:3n-3 was oxidized at the terminal pentadiene (C-10 to C-14) to the *bis*-allylic hydroperoxide at C-12 (n-5) and two *cis-trans*-conjugated hydroperoxides at C-14 (n-3) and C-10 (n-7). The penultimate pentadiene (C-7 to C-11) was oxidized to a *cis-trans*-conjugated hydroperoxide at C-11 (n-6), and this hydroperoxide, 11*R*-HPHTrE, was partly transformed to 11-ketohexadecatrienoic acid (11-KHTrE), as

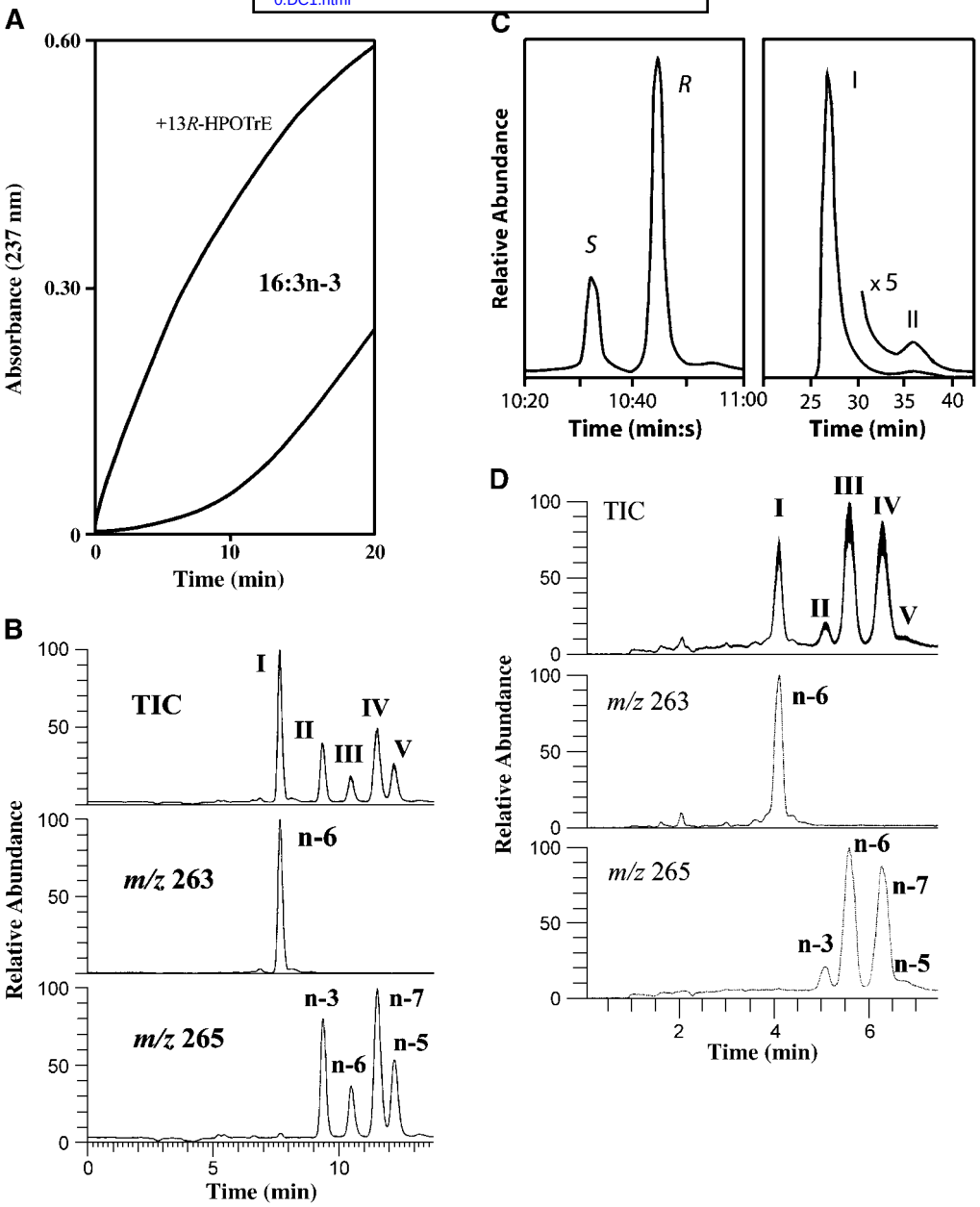

Fig. 1. Oxidation of 16:3n-3 by manganese lipoxygenase (Mn-LO) and Mn-LO G316A. A: The ultraviolet (UV) traces (237 nm) show the oxidation of 50 μM 16:3n-3 by Mn-LO (10 nM) with or without 10 μM 13*R*-hydroperoxyoctadecatrienoic acid (13*R*-HPOTrE) (top trace with 13*R*-HPOTrE). B: Normal-phase (NP)-HPLC-MS/MS analysis of the oxygenation products formed by Mn-LO upon incubation with 16:3n-3 and 13*R*-HPOTrE. Top trace, total ion current (TIC); middle trace, *m/z* 263→full scan, for detection of ketohexadecatrienoic acid (KHTrE); bottom trace, *m/z* 265→full scan, for detection of hydroxyhexadecatrienoic acid (HHTrE). Peak I contained 11-KHTrE, whereas peaks II–V contained hydroxy metabolites at the n-3, n-6, n-7, and n-5 positions (14-HHTrE, 11-HHTrE, 10-HHTrE, and 12-HHTrE), respectively. The NP-HPLC column was eluted with 3% isopropanol in hexane with 0.05 ml of acetic acid per liter (0.3 ml/min). C: Steric analysis of 14-HHTrE (left) and 10-HHTrE (right). The 2*S*-phenylpropionic acid derivatives of methylated and hydrogenated 14-HHTrE were separated by GC and analyzed by electron-impact mass spectrometry. The chromatogram shows single-ion monitoring (*m/z* 269); the *S* diastereoisomer elutes before the *R* diastereoisomer (42). 10-HHTrE was analyzed by chiral phase (CP)-HPLC (Chiralcel OB). 10-HHTrE was separated into a major component (peak I) and a minor component (peak II), which likely contained the *S* and *R* stereoisomers of 10-HHTrE, respectively, in analogy with separation of the *S* and *R* stereoiosmers of 11-hydroxyeicosatetraenoic acid (11-HETE) (cf. Fig. 5B). D: NP-HPLC-MS/MS analysis of the oxygenation products formed by Mn-LO upon incubation with 16:3n-3 and 13*R*-HPOTrE. The shorter retention times were attributable to regeneration of the NP-HPLC column, which was eluted as in B.

illustrated by NP-HPLC-MS/MS analysis of the products after TPP reduction (Fig. 1B). Steric analysis of the *cis-trans*-conjugated hydroperoxides was consistent with O_2 insertion from the same side of the terminal pentadiene, as 14-HPHTrE had mainly *R* configuration (~78% *R*) and 10-HPHTrE had mainly *S* configuration (>97% *S*) (Fig. 1C). In analogy with the oxidation of 18:2n-6 to the *bis*-allylic product 11*S*-HPODE (16), 12-HPHTrE might be formed as the *S* stereoisomer, but this was not investigated. The oxidation of 16:3n-3 by Mn^{III}-LO is summarized in **Fig. 2**.

Mn-LO G316A oxygenated 16:3n-3 in the presence of 13*R*-HPOTrE to three main products, which were identified after TPP reduction as 11-KHTrE, 11-hydroxyhexadecatrienoic acid (11-HHTrE), and 10-HHTrE (Fig. 1D). 11-HHTrE could be detected during the phase of rapid oxygenation but could be almost quantitatively transformed to 11-KHTrE, as judged from prolonged incubation times. 14-HHTrE was also formed, but the ratio of 14-HHTrE to 10-HHTrE was only 1:6 compared with 1:1.4 during Mn-LO oxidation. Finally, traces of 12-HHTrE were detected (<5% of 10-HHTrE). We conclude that the G316A mutation shifted the oxygenation of the terminal pentadiene from C-12 and C-14 toward C-10 and augmented the oxidation of the penultimate pentadiene at C-11 (but not as far as to C-9).

19:3n-3. Mn^{III}-LO oxidized only the penultimate pentadiene (C-10 to C-14) of 19:3n-3 and formed approximately equal amounts of the *cis-trans*-conjugated hydroperoxide at C-14 (14-HPNTrE) and the *bis*-allylic hydroperoxide at C-12 (12-HPNTrE) (NP-HPLC-MS/MS analysis after TPP reduction). Small amounts of 10-HPNTrE were also formed. On NP-HPLC, the elution order was 14-ketononadecatrienoic acid (14-KNTrE) (6 min), 14-hydroxynonadecatrienoic acid (14-HNTrE; 7 min), 12-HNTrE (8 min), and 10-HNTrE (9.5 min). 14*R*-HPNTrE was transformed to 14-KNTrE, whereas the other two hydroperoxides (10-HPNTrE and 12-HPNTrE) accumulated. CP-HPLC analysis (Chiralcel OB) showed that 14*S*-HNTrE eluted before the 14*R*-HNTrE stereoisomer and that Mn-LO formed 85% of the 14*R* stereoisomer (data not shown).

Mn^{III}-LO G316A augmented the formation of 10-HPNTrE so that 14-, 12-, and 10-HPNTrE were formed in a ratio of ~2:1:2 (NP-HPLC-MS/MS and UV analysis). The products formed by Mn-LO G316A were separated by CP-HPLC, as shown in **Fig. 3**. The most abundant stereo-

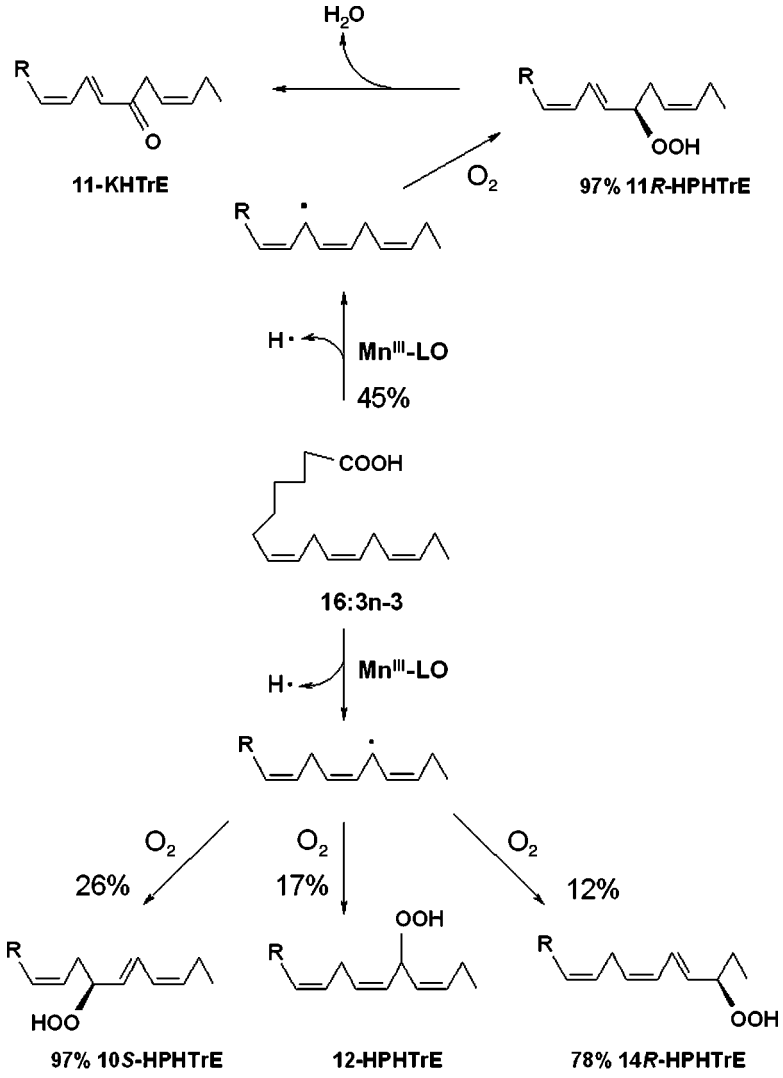

Fig. 2. Summary of the oxygenation of 16:3n-3 by Mn-LO. Hydrogen abstraction at the n-8 carbon is followed by oxygenation at the n-6 carbon (11*R*-HHTrE) and dehydration to the keto compound, 11-KHTrE (top). Hydrogen abstraction at the n-5 carbon is followed by the insertion of oxygen at positions n-7, n-5, and n-3 to yield 10*S*-HHTrE, 12-HHTrE, and 14-HHTrE, respectively. The relative amounts of the metabolites were assessed by their total ion intensities during MS/MS analysis. 11-KHTrE was apparently formed by the hydroperoxide isomerase activity of Mn-LO (17).

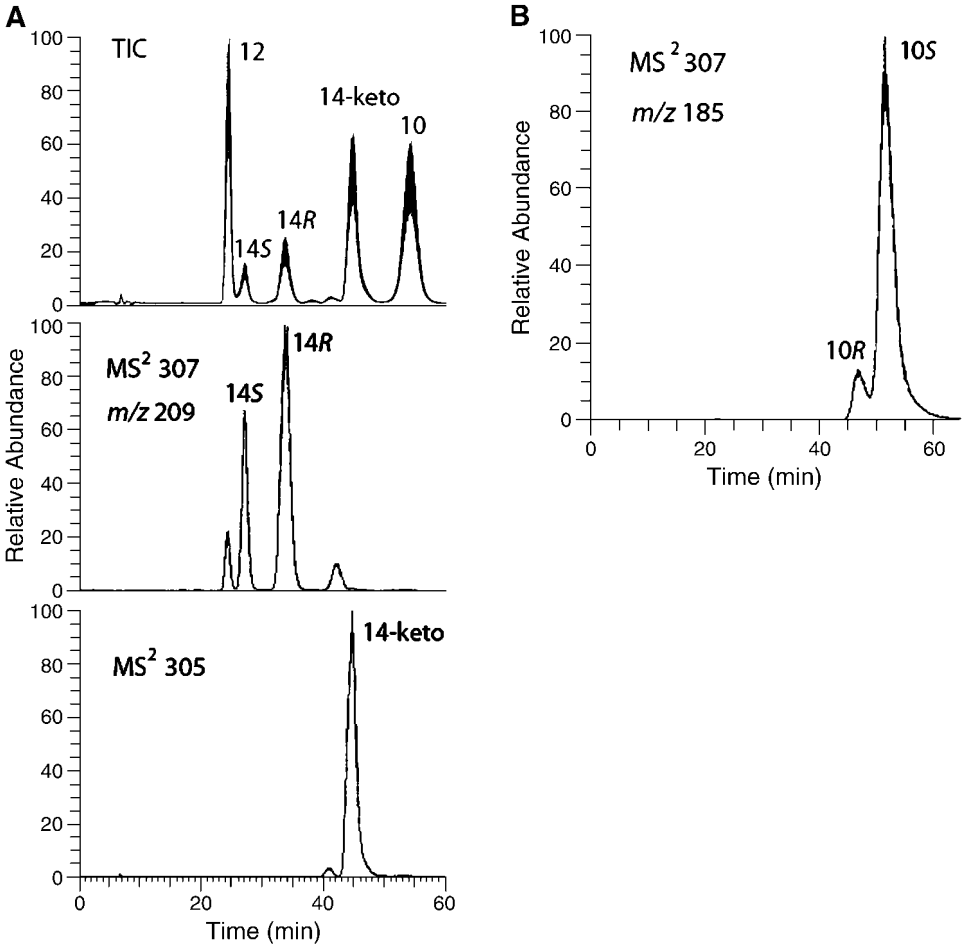

Fig. 3. Separation of 19:3n-3 metabolites on CP-HPLC with steric analysis of 14-hydroxynonadecatrienoic acid (14-HNTrE) and 10-HNTrE. A: The products formed from 19:3n-3 by Mn-LO G316A were separated on Chiralcel OB as shown by MS/MS analysis. Top trace, total ion current (TIC); middle trace, MS/MS analysis (*m/z* 307→full scan) with monitoring of *m/z* 209 (characteristic of 14-HNTrE); bottom trace, MS/MS analysis (*m/z* 305→full scan) for detection of ketononadecatrienoic acid. The numbers refer to the positions of the hydroxyl group: 10, 10-HNTrE; 12, 12-HNTrE; 14, 14-HNTrE. The separation of the 14-HNTrE stereoisomers suggested that the *R* stereoisomer was formed in some excess of the *S* stereoisomer by G316A. B: Separation of the *R* and *S* stereoisomers of 10-HNTrE by CP-HPLC (Chiralcel OD). The elution order, *S* before *R*, was deduced from the consistent elution order of stereoisomers of HODE and HETE on Chiralcel OD (35).

isomers were 14*R*-HNTrE and 10*S*-HPNTrE, but significant amounts of the two antipodes were also detected. We conclude that oxygenation was increased at C-10 by G316A compared with the native enzyme.

20:3n-3. This fatty acid was oxygenated by Mn^{III}-LO at the penultimate pentadiene (C-11 to C-15) to 15-HPETrE and 13-HPETrE in a ratio of ~3:2 as major products and to small amounts of 11-HPETrE (NP-HPLC-MS/MS analysis of alcohols). UV and LC-MS/MS analyses indicated that 11-HETrE eluted on the right shoulder of 13-HETE, and the amount of 11-HETrE was ~5% of the total products. 13-HPETrE accumulated as an end product even after prolonged incubation (60 min).

Mn^{III}-LO G316A transformed 15-HPETrE to 15-ketoeicosatrienoic acid (15-KETrE) and changed the relative amounts of 11-, 13-, and 15-HPETrE in analogy with the oxidation of 19:3n-3 at C-10, C-12, and C-14. UV analysis suggested that 11- and 15-HETrE were formed in a ratio of 4:1. Taking into account that 15-HPETrE was partly converted to 15-KETrE, the ratio of total oxidation at C-11 and C-15 was ~2:1. The relative amount of 13-HETrE was difficult to evaluate, as 11-HETrE had only a slightly longer retention time than 13-HETrE on NP-HPLC. The intensities of the specific 13-HETrE signal (*m/z* 225) and the 11-HETrE signal (*m/z* 199) suggested that these two metabolites were formed at approximately the same order of magnitude. We conclude that G316A clearly shifted the oxygenation from C-15 toward C-11 and C-13.

20:4n-6. Mn^{III}-LO oxygenated 20:4n-6 at C-11, C-13, and C-15. The UV time curve for the analysis of *cis-trans*-conjugated products with and without 13*R*-HPOTrE is shown in **Fig. 4A**, and the oxidation rate at different con-

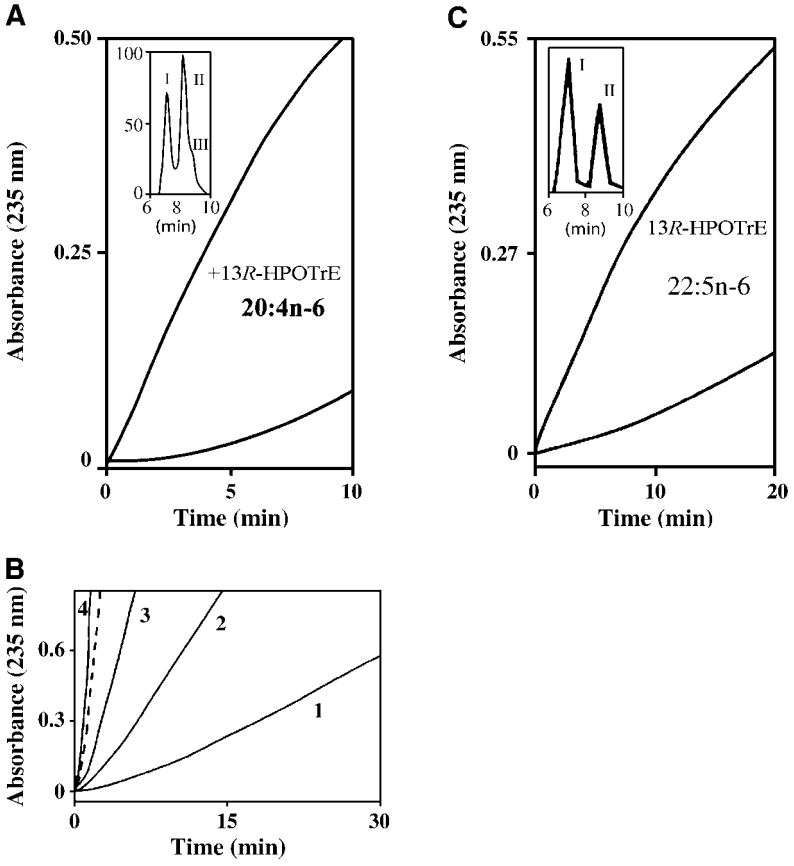

Fig. 4. Oxidation of 20:4n-6 and 22:5n-6 by Mn^{III}-LO. A: Time curve for the transformation of 20:4n-6 by Mn-LO (10 nM) with and without 10 μM 13*R*-HPOTrE to *cis-trans*-conjugated products with UV absorption at 235 nm. The inset shows reverse-phase (RP)-HPLC analysis of metabolites formed from 20:4n-6. 13-Hydroperoxyeicosatetraenoic acid (13-HPETE) eluted in peak I, and a mixture of 15-HETE and 11-HETE eluted in peak II, with 11-HETE (marked III) on the right shoulder of peak II. B: Oxidation of 50 μM 20:4n-6 by Mn-LO at different concentrations: 18 nM (trace 1), 55 nM (trace 2), 165 nM (trace 3), and 0.86 μM (trace 4). The dashed line shows, for comparison, the oxygenation of 50 μM 18:3n-3 by 18 nM Mn-LO. C: Transformation of 22:5n-6 by 10 nM Mn-LO with and without 10 μM 13*R*-HPOTrE. The inset shows NP-HPLC separation and MS/MS analysis of the two products after triphenylphosphine (TPP) reduction. Peak I contained the 17-hydroxy metabolite, and peak II contained the 15-hydroxy metabolite (see Table 2).

centrations of Mn-LO (0.018–0.860 μM) is shown in Fig. 4B. The maximal rate of oxidation of 50 μM 20:4n-6 with 55 nM Mn-LO to chromatophores at 235 nm was 0.068 absorbance units per minute [~7% of the oxidation rate of 18:3n-3 (7)]. The products were first analyzed by RP-HPLC-MS/MS after TPP reduction (see Table 2 below). On RP-HPLC, 13-HETE (peak I) eluted before 15-HETE (peak II), whereas 11-HETE (peak III; inset in Fig. 4A) eluted on the right shoulder of 15-HETE. On NP-HPLC, 13-HETE eluted between 15-HETE (5 min) and 11-HETE (7 min) with baseline separation (data not shown). The corresponding hydroperoxides eluted in the same order.

At the mid point of oxidation, 15*R*-HETE, 13-HETE, and 11*R*-HETE constituted ~60, 37, and 3% of the HETEs (integration of the signal intensity of the carboxylate anions at *m/z* 319 after reduction with TPP). Steric analysis of 15-HETE by CP-HPLC (Pirkle column) showed that 15*R*-HETE was formed as the main stereoisomer (at least >95%) (**Fig. 5A**). 11-HETE was a minor product, which was purified by NP-HPLC, analyzed by CP-HPLC as shown in Fig. 5B, and identified as the *R* stereoisomer. This suggested that a small fraction of 20:4n-6 might be bound to Mn-LO in the opposite "head-to-tail" configuration.

13-HPETE could only be detected by MS/MS analysis during the oxidation phase, with an increasing UV absorption at 235 nm, and not at the end. 13-HPETE was isolated by NP-HPLC and incubated with Mn-LO, and the products were analyzed. 13-HPETE was isomerized by Mn-LO to products with UV absorption at 235 nm (13-HPETE was converted by 0.4 μM Mn-LO to 5 μM 15-HPETE at a rate of 0.14 absorbance units per minute). NP-HPLC-MS/MS analysis demonstrated that 96% 15-HPETE and 4% 11-HPETE were formed. The oxidation of 20:4n-6 is summarized in **Fig. 6**.

20:4n-6 was not oxidized by Mn-LO G316A even in the presence at 5 μM 13*R*-HPOTrE, as judged from UV analysis.

22:5n-6 and 22:5n-3. Mn^{III}-LO oxygenated 22:5n-6, albeit slowly, as shown in Fig. 4C. The two major products were baseline separated by NP-HPLC and identified as the n-6 and n-8 hydroxy fatty acids after TPP reduction. Mn^{III}-LO also oxygenated 22:5n-3 at the n-6 and n-8 carbons, and both hydroperoxides accumulated as end products.

Oxygenation of dilinoleoyl-GPC

The UV trace (235 nm) from the oxidation of 125 μM dilinoleoyl-GPC by sLO-1 (~0.4 μM; 37 μg protein/ml in 0.1 M $NaBO_3$ buffer, pH 9.0) and Mn-LO (0.9 μM in 0.075 M $NaBO_3$ buffer, pH 9.0) is shown in **Fig. 7**. Mn-LO oxidized this phospholipid to UV-absorbing material with a UV maximum at 235 nm (inset in Fig. 7), suggesting the biosynthesis of *cis-trans*-conjugated hydroperoxides at a rate of 2 μmol/μmol Mn-LO/min. The products formed by Mn-LO at the linear oxidation phase were analyzed by NP-HPLC-MS/MS with UV detection after reduction with $NaBH_4$ and hydrolysis with 0.5 M KOH in methanol-water (10:1; overnight at 22°C). The main products were *cis-trans*-conjugated 13-HODE (52%) and 9-HODE (23%).

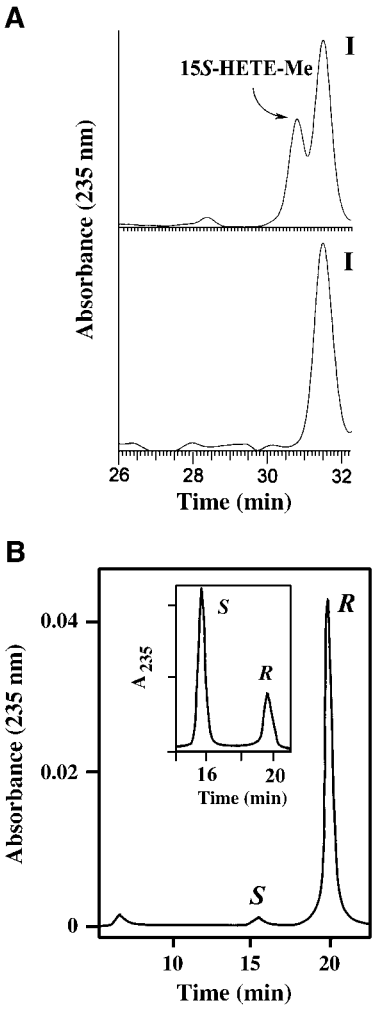

Fig. 5. Steric analysis by CP-HPLC of 15-HETE and 11-HETE formed from 20:4n-6 by Mn-LO. A: Methyl (Me) 15*S*-HETE was added to the methylated 15-HETE stereoisomer (in peak I) formed by Mn-LO in the top chromatogram; the bottom chromatogram shows the analysis of the formed 15-HETE stereoisomer. B: The chromatogram shows the separation by CP-HPLC (Chiralcel OB) of 11*S*-HETE and 11*R*-HETE stereoisomers formed by Mn^{III}-LO (marked *S* and *R*). The inset shows chromatography of the same sample after the addition of authentic 11*S*-HETE.

11-HODE could not be detected, but significant amounts of *trans-trans*-conjugated 13-HODE (14%) and 9-HODE (10%) were present (UV maximum at 230 nm).

UV analysis

The *cis-trans*-conjugated hydro(pero)xy fatty acids discussed below showed distinct UV maxima at 235–237 nm, whereas all of the n-8 and n-5 *bis*-allylic hydroperoxy fatty acids lacked UV absorption maxima in this region. Keto fatty acids with the 1-keto-2*E*,4*Z*-pentadiene element showed distinct UV maxima at 275–277 nm.

MS analysis

The MS/MS spectra of the major products are summarized in **Tables 1 and 2**, and the MS/MS spectra are interpreted in the supplementary data available online. General features of the MS/MS spectra will be discussed here.

MS/MS analysis of hydroperoxy fatty acids yields a strong signal attributable to loss of water, and the hydroperoxides are also partly dehydrated to the keto compounds in the heated capillary (200–325°C) of the mass spectrometer (44–46). The MS/MS/MS spectra of hydroperoxides are virtually identical to the MS/MS spectra of the corresponding keto fatty acids. Keto fatty acids are subject to keto-enol tautomerism, and their MS/MS spectra are more difficult to interpret than the MS/MS spectra of hydroxy fatty acids (47). The MS/MS/MS spectra of hydroperoxides formed from 16:3n-3 are summarized in Table 1. For identification, the hydroperoxy fatty acids were reduced to hydroxy fatty acids with TPP (or $NaBH_4$). The MS/MS spectra of hydroxy and keto fatty acids formed from 16:3n-3 are presented in **Fig. 8**. 13-HETE was identified previously as a cytochrome P450 metabolite (48). The MS analyses of 13-HPETE, 13-ketoeicosatetraenoic acid (13-KETE), and octadeuterated 13-HPETE are summarized in **Fig. 9**.

MS/MS analysis of the *bis*-allylic hydroxy fatty acid at the n-8 and n-5 positions showed characteristic signals attributable to α-cleavage at the oxidized carbon (Table 2). The n-8 hydroxy fatty acids showed loss of 98 amu (H_2C=CH-C_5H_{11}) and 96 amu(H_2C=CH-C_5H_9) from A^- of the n-6 and n-3 fatty acids, respectively, whereas 12-HHTrE (n-5) showed a characteristic signal attributable to loss of 56 amu (H_2C=CH-C_2H_5). The relative amounts of hydroperoxides at the n-8 carbon varied from trace amounts (17:3n-3) to 40–50% of total products (19:3n-3, 20:3n-3, 22:5n-3, and 22:5n-6), as judged from MS/MS analysis of products at the middle part of the oxidation curves.

19:3n-3, 20:3n-3, and 20:4n-6 were oxidized at the n-10 carbon, and the MS/MS spectra of the corresponding hydroxy fatty acids showed intense signals at *m/z* 185 [$^-$OOC-$(CH_2)_8$-CHO; 35% of base peak], *m/z* 199 [$^-$OOC-$(CH_2)_9$-CHO; 27%], and *m/z* 167 (loss of CHO-CH=CH-CH = CH-C_5H_{11}; 60%), respectively (Table 2). 10-HHTrE yielded a characteristic fragment at *m/z* 183 [$^-$OOC-$(CH_2)_5$-CH=CH-CH_2-CHO]. The MS/MS spectra of the *cis-trans*-conjugated metabolites with a hydroxyl group at the n-6 carbons showed characteristic signals attributable to loss of 100 amu (HCO-C_5H_{11}) or 98 amu (HCO-C_5H_9) from the carboxylate anion (A^-) of n-6 and n-3 fatty acids, respectively (45).

Extraction of manganese

Kariapper, Dunham, and Funk (36) reported that iron could be reversibly extracted from sLO-3 with an anion-chelating resin (Chelex-100) in 0.1 $NaHCO_3$ buffer (pH 8.0)/0.1 M NaCl. We assessed whether this method could be used to reconstitute the Mn-LO apoprotein with manganese from Mn-LO. The results are presented in the supplementary data. We found that manganese can be extracted from Mn-LO in some analogy with iron extraction from sLO-3 in $NaHCO_3$ buffer with Chelex-100, but this required increased temperatures only 8–9°C below its thermal inactivation. A series of attempts to reconstitute this apo-

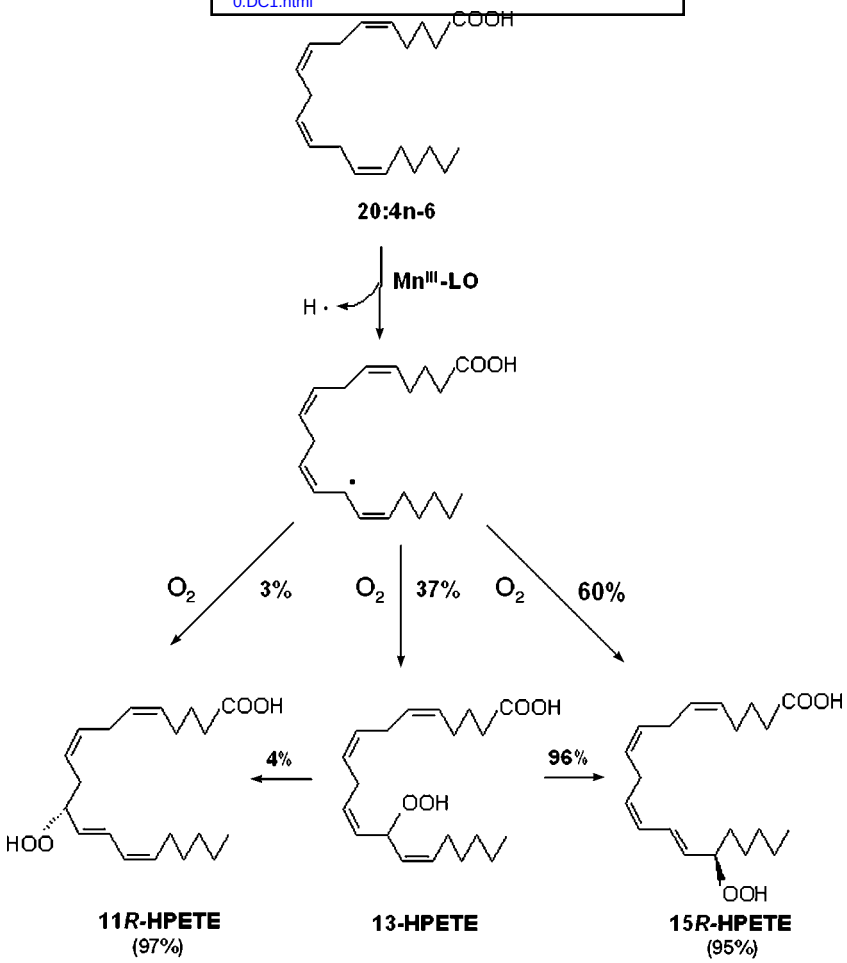

Fig. 6. Overview of the products formed from 20:4n-6 by Mn-LO. The reaction proceeds with the formation of an alkyl radical followed by the insertion of oxygen at positions n-10, n-8, and n-6, yielding 11*R*-HPETE, 13-HPETE, and 15*R*-HPETE, respectively. The absolute configurations of 15-HPETE and 11-HPETE (*R* and *R*, respectively) suggest that a small fraction of 20:4n-6 might bind in opposite directions in the active site. The absolute configuration of 13-HPETE was not determined, but the *S* stereoisomer is likely the main product, in analogy with the oxidation of 18:2n-6 (16).

protein with 10 μM Mn^{2+} or with Mn^{3+} [from a 1 mM suspension of Mn(III)-acetate-dihydrate (Merck) at different incubation times and temperatures] were unsuccessful. Extraction of Mn presumably led to irreversible denaturation.

DISCUSSION

Our main findings are that Mn-LO oxidizes dilinoleoyl-GPC and C_{16} to C_{22} n-3 and n-6 fatty acids in agreement with a tail-first model and forms a series of novel *bis*-allylic hydroperoxy C_{16}, C_{20}, and C_{22} fatty acids. These observations have implications for the biological function of Mn-LO during the infection process of *G. graminis*. The hyphae of *G. graminis* penetrate the root systems of wheat and other grasses (14) and can secrete Mn-LO. Mn-LO may oxidize fatty acids in the invaded root tissues and generate hydroperoxides and reactive oxygen species. The importance of Mn-LO during the infection process of *G. graminis* will merit further studies.

Dilinoleoyl-GPC was oxidized by Mn-LO, albeit slowly. This implies a tail-first alignment (13, 33). The oxygenation of the n-3 fatty acids with 16 to 19 carbons can be explained in a logical context, if we assume that their carboxyl groups are bound at a fixed position, allowing oxidation closer to the carboxyl group of 16:3n-3 and 17:3n-3 and closer to the ω-end of 18:3n-3 and 19:3n-3. The carboxyl group of fatty acids likely interacts with charged amino acids of coral 8*R*-LOX in a tail-first model (12). The nature of this interaction of the substrates with Mn-LO is unclear. As 22:5n-3, 22:5n-6, 20:3n-3, and 20:4n-6 were oxidized by Mn-LO at the n-6 and n-8 positions in the same way as 19:3n-3, an alternative hypothesis could be that the ω-end of 20 and 22 carbon substrates slides into the catalytic site irrespective of the specific binding of their carboxyl groups.

16:3n-3 occurs in plant tissues and is a precursor to dinor-oxophytodienoic acid (49). This report shows that it can be oxygenated by Mn^{III}-LO into four hydroperoxy fatty acids: 11*R*-HPHTrE by oxidation of the penultimate 1*Z*,

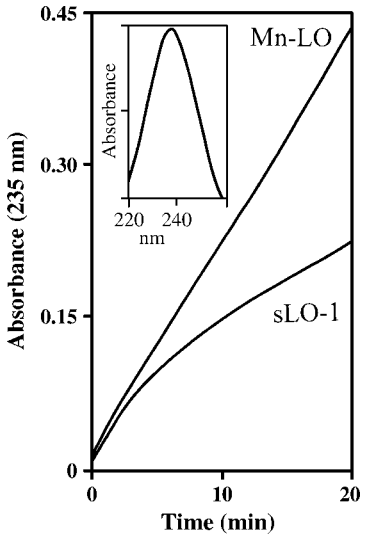

Fig. 7. UV analysis of the oxidation of dilinoleoyl-glycerophosphatidylcholine (GPC) by soybean lipoxygenase-1 (sLO-1) and by Mn-LO. The kinetic traces of UV absorbance at 235 nm show the oxygenation of dilinoleoyl-GPC (125 μM) with ~0.4 μM sLO-1 and ~0.9 μM Mn-LO to *cis-trans*-conjugated hydroperoxyoctadecadienoic acid (HPODE). The inset shows the UV spectrum (220–260 nm) of the products formed by Mn-LO.

4*Z*-pentadiene, and 10*S*-HPHTrE, 12-HPHTrE, and 14-HPHTrE (78% *R*) by oxidation of the terminal 1*Z*,4*Z*-pentadiene. The product analysis supported the notion that hydrogen abstraction occurred at the n-8 and n-5 carbons in approximately equal amounts, followed by O_2 insertion at C-11 and at C-10, C-12, and C-14 (Fig. 2). The ratio of 10-HPETE to 14-HPETE was ~1.4:1. This appears to be the first example of lipoxygenation of the terminal 1*Z*,4*Z*-pentadiene of a naturally occurring n-3 fatty acid. For comparison, sLO-1 oxidized 16:3n-3 to a singular product, 11*S*-HPHTrE, but this enzyme is also known to oxygenate 18:2n-2 to 17-HPODE (28, 29).

Mn-LO G316A clearly oxidized carbons of 16:3n-3, 19:3n-3, and 20:3n-3 closer to the carboxyl group than Mn-LO. Thus, Mn-LO G316A facilitated the oxygenation of 16:3n-3 at the n-7 position over the n-3 position and facilitated the oxygenation of 19:3n-3 and 20:3n-3 at the n-10 and n-8 positions over the n-6 position. Mn-LO G316A oxygenated 18:3n-3 and 18:2n-6 in essentially the same way as Mn-LO, with only a marginal increase in the oxidation at C-9 (17).

It is interesting to compare Mn-LO G316A with the corresponding Gly→Ala mutations of 8*R*-LOX and 12*R*-LOX, which converted 8*R*-LOX to a 12*S*-lipoxygenase and 12*R*-LOX to an enzyme with 12*R*- and 8*S*-lipoxygenase activities (32). The Gly→Ala mutation of Mn-LO changed oxygenation with additional positional accuracy, as Mn-LO G316A also influenced the oxygenation of *bis*-allylic carbons at the n-8 position of 19:3n-3 and 20:3n-3 as well as the oxygenation of carbons at n-10. The shift in oxygenation of 20:3n-3 by Mn-LO G316A is in the same direction as the shift of 20:4n-6 oxidation by the Gly→Ala mutation of 12*R*-LOX and in the opposite direction to this mutation of 8*R*-LOX (34). 12*R*-LOX may bind the substrate with the carboxyl group embedded in the active site (head-first), whereas 8*R*-LOX and Mn-LO likely bind fatty acids in the opposite direction (tail-first). Yet, the Gly→Ala mutation of Mn-LO and 8*R*-LOX shifted the oxygenation in differ-

TABLE 1. LC-MS/MS/MS analysis of hydroperoxy fatty acids formed from 16:3n-3 by Mn-LO

Product	Position of the OOH group	Key ions observed in MS/MS/MS spectra[a] (relative abundance in % of base-peak)
14-HPHTrE	n-3	245 (25), 219 (100), 191 (40), 165 (18), 135 (12)
12-HPHTrE	n-5	45 (45), 219 (100), 201 (5), 165 (5), 163 (38), 137 (2)
11-HPHTrE	n-6	245 (26), 219 (100), 201 (4), 165 (6), 149 (22), 111 (18)
10-HPHTrE	n-7	245 (45), 219 (100), 205 (8), 202 (4), 165 (8), 125 (14)

HPHTrE, hydroperoxyhexadecatrienoic acid; Mn-LO, manganese lipoxygenase.
[a] Spectra were recorded at *m/z* 281→*m/z* 263→full scan. The hydroperoxides were isolated, reduced with triphenylphosphine, and identified by LC-MS/MS analysis. The MS/MS/MS spectrum of 11-HPHTrE was virtually identical to the MS/MS spectrum of 11-ketohexadecatrienoic acid (Fig. 8A).

TABLE 2. LC-MS/MS analysis of hydroxy fatty acids formed by Mn-LO substrate position of the hydroxyl group (carbon) key ions observed in MS/MS spectra (relative abundance in % of base-peak)

Substrate	Position of hydroxyl group (carbon)	Key ions observed in MS/MS spectra (relative abundance in % of base-peak)
17:3n-3	n-6 (C-12)	261 (100), 235 (30), 217 (20), 181 (60), 113 (3)[a]
19:3n-3	n-6 (C-14)	289 (100), 263 (25), 238 (35), 209 (40), 193 (25), 165 (7), 113 (7)[a]
	n-8 (C-12)	289 (100), 263 (30), 211 (80), 191 (30), 165 (40), 111 (5)[b]
	n-10 (C-10)	289 (100), 263 (3), 245 (3), 211 (5), 199 (12), 185 (35)
20:3n-3	n-6 (C-15)	303 (100), 293 (8), 277 (8), 252 (45), 224 (40), 223 (40), 207 (18), 195 (5), 113 (5)[a]
	n-8 (C-13)	303 (100), 277 (10), 225 (50), 205 (15), 179 (15), 141 (4)[b]
	n-10 (C-11)	303 (100), 277, 213 (6), 199 (27)
20:4n-6	n-6 (C-15)	301 (100), 275 (20), 257 (35), 219 (40), 175 (25), 113 (5)[c]
	n-8 (C-13)	301 (90), 275 (55), 257 (25), 193 (100), 177 (10), 149 (8)[d]
	n-10 (C-11)	301 (100), 275 (60), 257 (30), 221 (7), 193 (15), 167 (60), 149 (3)[e]
22:5n-3	n-6 (C-17)	327 (100), 301 (10), 283 (30), 247 (30), 203 (5)
	n-8 (C-15)	327 (100), 301 (20), 283 (30), 249 (20), 221 (60)
22:5n-6	n-6 (C-17)	327 (100), 301 (35), 283 (45), 245 (35), 201 (45)
	n-8 (C-15)	327 (100), 301 (60), 283 (55), 247 (10), 219 (75)

HETE, hydroxyeicosatetraenoic acid.
[a] Fragmentation pattern similar to 13-hydroxyoctadecatrienoic acid reported previously (17, 46).
[b] Fragmentation pattern similar to 11-hydroxyoctadecatrienoic acid reported previously (46).
[c] Fragmentation pattern similar to 15-HETE reported previously (45).
[d] Fragmentation pattern similar to 13-HETE reported previously (48).
[e] Fragmentation pattern similar to 11-HETE reported previously (45).

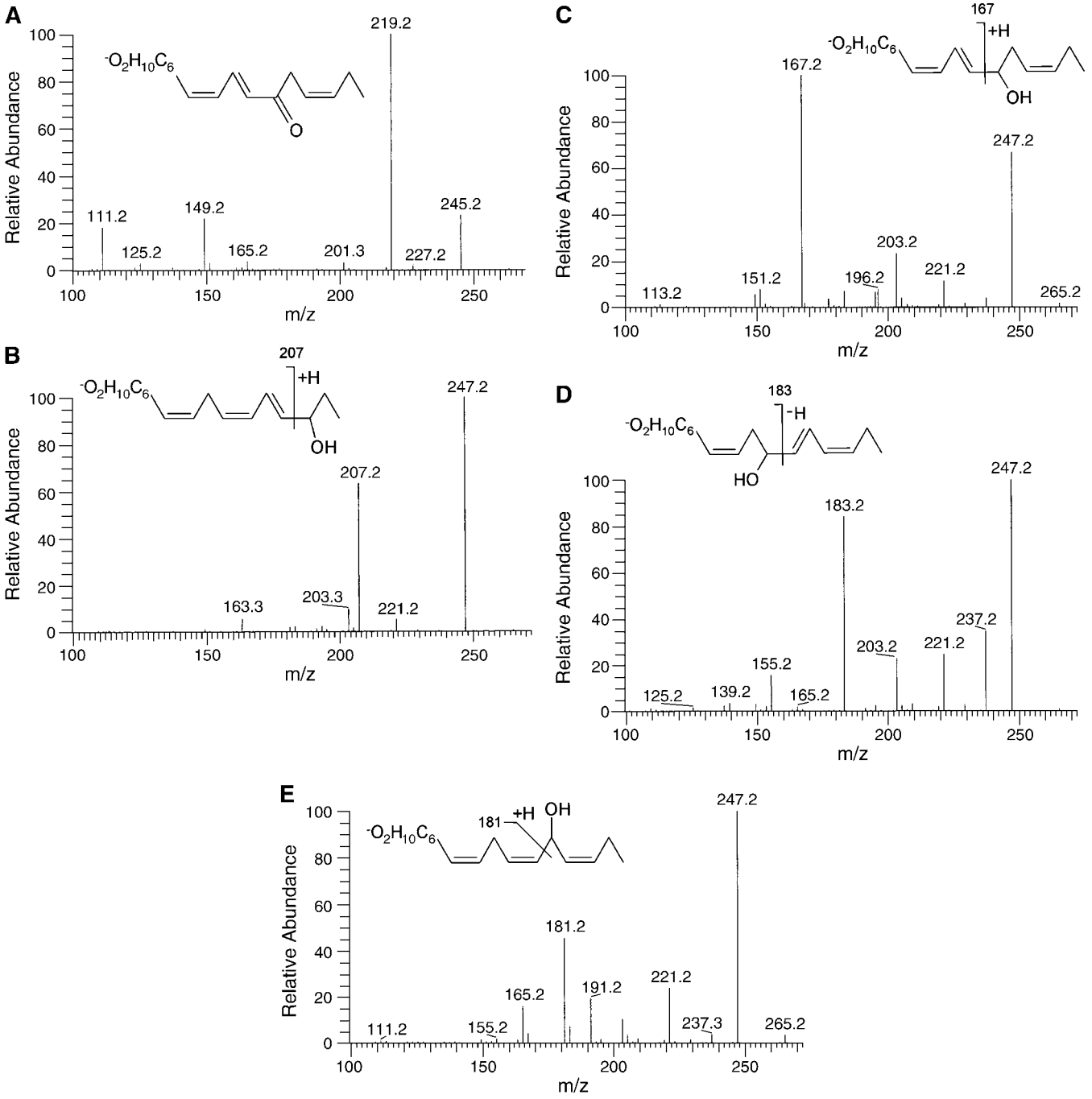

Fig. 8. NP-HPLC-MS/MS analysis of oxygenated metabolites of 16:3n-3 formed by Mn^{III}-LO. A: MS/MS analysis (*m/z* 265→full scan) of the material in peak I (Fig. 1B), which was found to contain 11-KHTrE. B: MS/MS analysis (*m/z* 265→full scan) of the material in peak II (14-HHTrE). C: MS/MS analysis (*m/z* 265→full scan) of the material in peak III (11-HHTrE). D: MS/MS analysis (*m/z* 265→full scan) of the material in peak IV (10-HHTrE). E: MS/MS analysis (*m/z* 265→full scan) of the material in peak V (12-HHTrE). The insets show the proposed structures and formation of major fragments during MS/MS analysis.

ent directions. The effect of the Gly→Ala mutations on 8*R*- and 12*R*-LOX was more pronounced than expected from frameshift repositioning of 20:4n-6 by one methylene unit, and Coffa and colleagues (32–34) suggested that the Ala residue is located near the entrance of the catalytic site and may shield the outer end of the 1*Z*,4*Z*-pentadiene from attack by O_2. Our results suggest that Ala316 may shield the inner end of the 1*Z*,4*Z*-pentadiene from attack by O_2 and may allow oxygenation at its outer end. This difference between Mn-LO and 8*R*-LOX may be related to their oxygenation mechanisms. Mn-LO catalyzes suprafacial hydrogen abstraction and oxygenation, whereas Fe-lipoxygenases have an antarafacial relationship (16, 33).

A remarkable feature of Mn-LOX is its capacity to form *bis*-allylic hydroperoxy fatty acids at the n-8 position or even at the n-5 position. A wide selection of Fe-lipoxygenases has

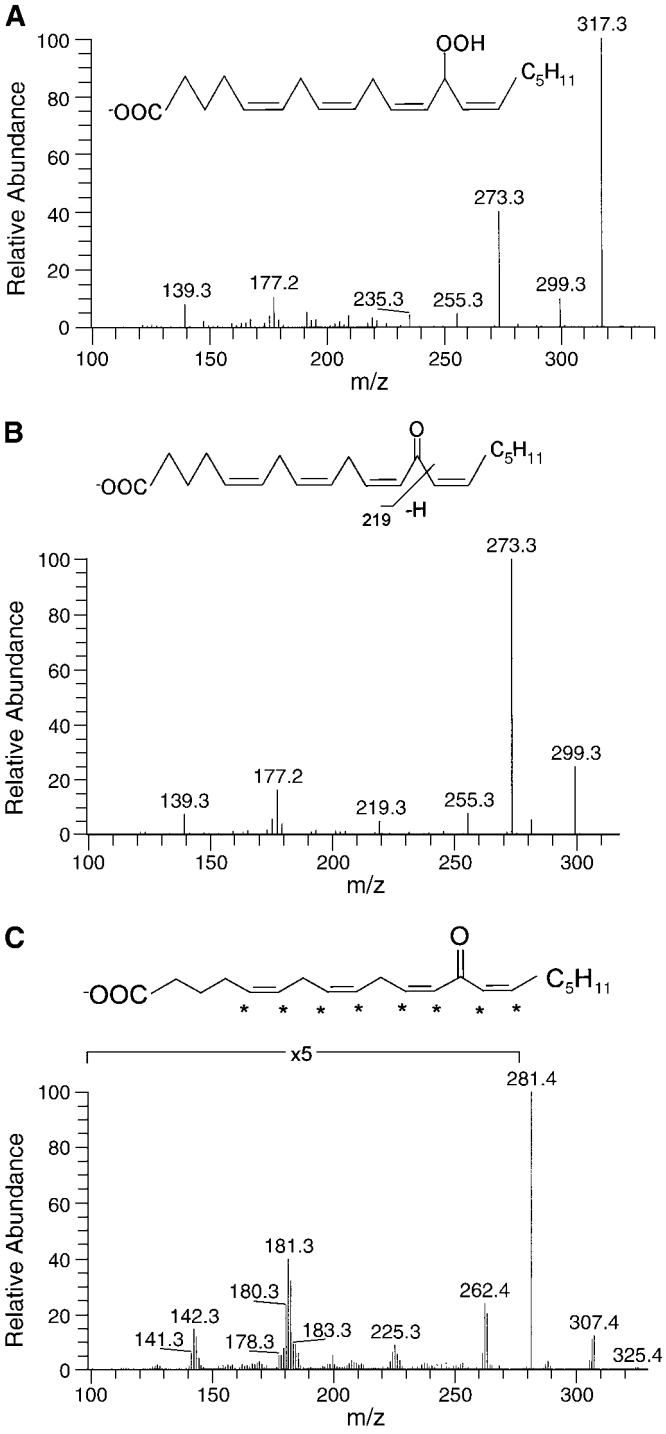

Fig. 9. Mass spectrometric analysis of 13-HPETE and [$^2H_8$]13-HPETE formed by Mn^{III}-LO. A: MS/MS analysis (*m/z* 335→full scan) of 13-HPETE. B: MS/MS analysis (*m/z* 31→full scan) of 13-ketoeicosatetraenoic acid (13-KETE), which was formed by dehydration of 13-HPETE in the ion trap (44, 46). C: MS/MS/MS analysis (*m/z* 343→*m/z* 324–325→full scan) of [5,6,8,9,11,12,14,15-$^2H_8$]13-HPETE. Deuterium is marked by asterisks in the structure at top, which shows the likely dehydration product, [5,6,8,9,11,12,14,15-$^2H_8$]13-KETE, formed by the analysis process.

been studied extensively with frameshift repositioning of substrates and by site-directed mutagenesis of the active sites (4). Yet, significant O_2 insertion at *bis*-allylic carbons of fatty acid substrates has not been reported. This difference could be due to *i*) steric factors influencing the distribution of the charge on carbon-centered radical ($L^{\bullet}$) and O_2 access to the radical (21), *ii*) catalytic metals, *iii*) the geometry of O_2 insertion, which is antarafacial to hydrogen abstraction in Fe-lipoxygenases and suprafacial in Mn-LO, and *iv*) the rapid conversion of the *bis*-allylic peroxyl radical to the *bis*-allylic hydroperoxide by Mn-LO. Many of these possibilities could be studied with a cambialistic lipoxygenase (active with either Fe or Mn), but this enzyme remains to be discovered or to be created by site-directed mutagenesis. We attempted to address the first two possibilities by preparing the apoprotein of Mn-LO for reconstitution with Mn and with Fe. Unfortunately, extraction of manganese seemed to result in irreversible denaturation of the enzyme.

The nonenzymatic oxidation of fatty acids to *bis*-allylic hydroperoxides is informative. 18:2n-6 is the prototype. Autoxidation of 18:2n-6 generates a small percentage of 11-HPODE, but in the presence of molar concentrations of an antioxidant, α-tocopherol, 9-HPODE, 11-HPODE, and 13-HPODE are formed in almost equal amounts (19). α-Tocopherol traps the 11-peroxyl radical, which is unstable and otherwise will undergo β-fragmentation (with the formation of 9- and 13-peroxyl radicals) at a rate of 1.9×10^6 s^{-1} (19). Mn-LO thus has the unique capacity to form the 11*S*-peroxyl radical of 18:2n-6 and to reduce the radical to the more stable product, 11*S*-HPODE, at a rate that apparently can compete with nonenzymatic β-fragmentation (16). This suggests that the biosynthesis of 11*S*-HPODE cannot simply be explained by O_2 access to C-11 of the pentadiene radical, as the 11-peroxyl radical is so short-lived. Fe-lipoxygenases may lack the ability to reduce *bis*-allylic peroxyl radicals to *bis*-allylic hydroperoxides at a compatible rate with β-fragmentation, except for the lipoxygenase domain of allene oxide synthase (23). Compared with Mn-LO, sLO-1 only slowly transforms 11-HPODE to *cis-trans*-conjugated HPODE (20).

20:3n-3 appeared to be metabolized in the same way as 20:4n-6 by Mn-LO, but there was one notable exception. 13-HPETrE accumulated, whereas 13-HPETE was converted to 15*R*-HPETE by Mn-LO. This presumably implies that Mn^{III}-LO can transform 13-HPETE (but not 13-HPETrE) to a peroxyl radical at C-13, part of which will undergo rapid β-fragmentation and isomerization to a peroxyl radical at C-15 and form 15*R*-HETE (19, 50). It should be possible to determine the structural basis for this difference between 13-HPETE and 13-HPETrE, as positional isomers of 20:4n-6 and 20:3n-3 are available.

In summary, we have found that Mn-LO likely binds fatty acids tail-first and can oxidize fatty acids with 16–22 carbons to *bis*-allylic and *cis-trans*-conjugated hydroperoxy fatty acids. These results can be explained by frameshift rearrangement with the catalytic base. Genes homologous to Mn-LO occur in *Aspergillus* and in the *Magnaporthaceae* family. Whether any of these putative lipoxygenases are

expressed and whether they contain Fe or Mn as catalytic metals are worthy of future studies, as additional Mn-LOs are needed to analyze the catalytic difference between Mn-LO and Fe-lipoxygenase.

This work was supported by Vetenskapsrådet medicin (03X-06523), Formas (222-2005-1733), and Magn. Bergvalls Stiftelse. The authors thank Dr. M. Hamberg (Karolinska Institutet, Stockholm, Sweden) and Dr. H. Kühn (University Medicine Berlin-Charité, Berlin, Germany) for generous advice.

REFERENCES

1. Brash, A. R. 1999. Lipoxygenases: occurrence, functions, catalysis, and acquisition of substrate. *J. Biol. Chem.* **274:** 23679–23682.
1a. Lütteke, T., P. Krieg, G. Fürstenberger, and C. W. von der Lieth. 2003. LOX-DB–database on lipoxygenases. *Bioinformatics.* **19:** 2482–2483.
2. Porta, H., and M. Rocha-Sosa. 2002. Plant lipoxygenases. Physiological and molecular features. *Plant Physiol.* **130:** 15–21.
3. Liavonchanka, A., and I. Feussner. 2006. Lipoxygenases: occurrence, functions and catalysis. *J. Plant Physiol.* **163:** 348–357.
4. Kuhn, H., J. Saam, S. Eibach, H. G. Holzhutter, I. Ivanov, and M. Walther. 2005. Structural biology of mammalian lipoxygenases: enzymatic consequences of targeted alterations of the protein structure. *Biochem. Biophys. Res. Commun.* **338:** 93–101.
5. Su, C., and E. H. Oliw. 1998. Manganese lipoxygenase. Purification and characterization. *J. Biol. Chem.* **273:** 13072–13079.
6. Hörnsten, L., C. Su, A. E. Osbourn, U. Hellman, and E. H. Oliw. 2002. Cloning of the manganese lipoxygenase gene reveals homology with the lipoxygenase gene family. *Eur. J. Biochem.* **269:** 2690–2697.
7. Cristea, M., Å. Engström, C. Su, L. Hörnsten, and E. H. Oliw. 2005. Expression of manganese lipoxygenase in *Pichia pastoris* and site-directed mutagenesis of putative metal ligands. *Arch. Biochem. Biophys.* **434:** 201–211.
8. Boyington, J. C., B. J. Gaffney, and L. M. Amzel. 1993. The three-dimensional structure of an arachidonic acid 15-lipoxygenase. *Science.* **260:** 1482–1486.
9. Minor, W., J. Steczko, B. Stec, Z. Otwinowski, J. T. Bolin, R. Walter, and B. Axelrod. 1996. Crystal structure of soybean lipoxygenase L-1 at 1.4 A resolution. *Biochemistry.* **35:** 10687–10701.
10. Skrzypczak-Jankun, E., L. M. Amzel, B. A. Kroa, and M. O. Funk, Jr. 1997. Structure of soybean lipoxygenase L3 and a comparison with its L1 isoenzyme. *Proteins.* **29:** 15–31.
11. Gillmor, S. A., A. Villasenor, R. Fletterick, E. Sigal, and M. F. Browner. 1997. The structure of mammalian 15-lipoxygenase reveals similarity to the lipases and the determinants of substrate specificity. *Nat. Struct. Biol.* **4:** 1003–1009.
12. Oldham, M. L., A. R. Brash, and M. E. Newcomer. 2005. Insights from the X-ray crystal structure of coral 8R-lipoxygenase: calcium activation via a C2-like domain and a structural basis of product chirality. *J. Biol. Chem.* **280:** 39545–39552.
13. Youn, B., G. E. Sellhorn, R. J. Mirchel, B. J. Gaffney, H. D. Grimes, and C. Kang. 2006. Crystal structures of vegetative soybean lipoxygenase VLX-B and VLX-D, and comparisons with seed isoforms LOX-1 and LOX-3. *Proteins.* **65:** 1008–1020.
14. Oliw, E. H. 2002. Plant and fungal lipoxygenases. *Prostaglandins Other Lipid Mediat.* **68–69:** 313–323.
15. van Leyen, K., R. M. Duvoisin, H. Engelhardt, and M. Wiedmann. 1998. A function for lipoxygenase in programmed organelle degradation. *Nature.* **395:** 392–395.
16. Hamberg, M., C. Su, and E. Oliw. 1998. Manganese lipoxygenase. Discovery of a bis-allylic hydroperoxide as product and intermediate in a lipoxygenase reaction. *J. Biol. Chem.* **273:** 13080–13088.
17. Cristea, M., and E. H. Oliw. 2006. A G316A mutation of manganese lipoxygenase augments hydroperoxide isomerase activity: mechanism of biosynthesis of epoxyalcohols. *J. Biol. Chem.* **281:** 17612–17623.
18. Gardner, H. W. 1989. Soybean lipoxygenase-1 enzymically forms both (9S)- and (13S)-hydroperoxides from linoleic acid by a pH-dependent mechanism. *Biochim. Biophys. Acta.* **1001:** 274–281.
19. Tallman, K. A., D. A. Pratt, and N. A. Porter. 2001. Kinetic products of linoleate peroxidation: rapid beta-fragmentation of nonconjugated peroxyls. *J. Am. Chem. Soc.* **123:** 11827–11828.
20. Oliw, E. H., M. Cristea, and M. Hamberg. 2004. Biosynthesis and isomerization of 11-hydroperoxylinoleates by manganese- and iron-dependent lipoxygenases. *Lipids.* **39:** 319–323.
21. Kitaguchi, H., K. Ohkubo, S. Ogo, and S. Fukuzumi. 2005. Direct ESR detection of pentadienyl radicals and peroxyl radicals in lipid peroxidation: mechanistic insight into regioselective oxygenation in lipoxygenases. *J. Am. Chem. Soc.* **127:** 6605–6609.
22. Knapp, M. J., F. P. Seebeck, and J. P. Klinman. 2001. Steric control of oxygenation regiochemistry in soybean lipoxygenase-1. *J. Am. Chem. Soc.* **123:** 2931–2932.
23. Boutaud, O., and A. R. Brash. 1999. Purification and catalytic activities of the two domains of the allene oxide synthase-lipoxygenase fusion protein of the coral *Plexaura homomalla*. *J. Biol. Chem.* **274:** 33764–33770.
24. Schilstra, M. J., G. A. Veldink, and J. F. Vliegenthart. 1994. The dioxygenation rate in lipoxygenase catalysis is determined by the amount of iron (III) lipoxygenase in solution. *Biochemistry.* **33:** 3974–3979.
25. Wang, Z. X., S. D. Killilea, and D. K. Srivastava. 1993. Kinetic evaluation of substrate-dependent origin of the lag phase in soybean lipoxygenase-1 catalyzed reactions. *Biochemistry.* **32:** 1500–1509.
26. Su, C., M. Sahlin, and E. H. Oliw. 2000. Kinetics of manganese lipoxygenase with a catalytic mononuclear redox center. *J. Biol. Chem.* **275:** 18830–18835.
27. Perez-Gilabert, M., I. Sanchez-Felipe, A. Morte, and F. Garcia-Carmona. 2005. Kinetic properties of lipoxygenase from desert truffle (*Terfezia claveryi* Chatin) ascocarps: effect of inhibitors and activators. *J. Agric. Food Chem.* **53:** 6140–6145.
28. Holman, R. T., P. O. Egwim, and W. W. Christie. 1969. Substrate specificity of soybean lipoxidase. *J. Biol. Chem.* **244:** 1149–1151.
29. Egmond, M. R., G. A. Veldink, J. F. Vliegenthart, and J. Boldingh. 1975. On the positional specificity of the oxygenation reaction catalysed by soybean lipoxygenase-1. *Biochim. Biophys. Acta.* **409:** 399–401.
30. Kuhn, H., H. Sprecher, and A. R. Brash. 1990. On singular or dual positional specificity of lipoxygenases. The number of chiral products varies with alignment of methylene groups at the active site of the enzyme. *J. Biol. Chem.* **265:** 16300–16305.
31. Kuhn, H. 2000. Structural basis for the positional specificity of lipoxygenases. *Prostaglandins Other Lipid Mediat.* **62:** 255–270.
32. Coffa, G., and A. R. Brash. 2004. A single active site residue directs oxygenation stereospecificity in lipoxygenases: stereocontrol is linked to the position of oxygenation. *Proc. Natl. Acad. Sci. USA.* **101:** 15579–15584.
33. Coffa, G., A. N. Imber, B. C. Maguire, G. Laxmikanthan, C. Schneider, B. J. Gaffney, and A. R. Brash. 2005. On the relationships of substrate orientation, hydrogen abstraction and product stereochemistry in single and double dioxygenations by soybean lipoxygenase-1 and its Ala542Gly mutant. *J. Biol. Chem.* **280:** 38756–38766.
34. Coffa, G., C. Schneider, and A. R. Brash. 2005. A comprehensive model of positional and stereo control in lipoxygenases. *Biochem. Biophys. Res. Commun.* **338:** 87–92.
35. Meruvu, S., M. Walther, I. Ivanov, S. Hammarström, G. Fürstenberger, P. Krieg, P. Reddanna, and H. Kuhn. 2005. Sequence determinants for reaction specificity of the murine 12(R)-lipoxygenase. Targeted substrate modification and site directed mutagenesis. *J. Biol. Chem.* **280:** 36633–36641.
36. Kariapper, M. S., W. R. Dunham, and M. O. Funk, Jr. 2001. Iron extraction from soybean lipoxygenase 3 and reconstitution of catalytic activity from the apoenzyme. *Biochem. Biophys. Res. Commun.* **284:** 563–567.
37. Graff, G., L. A. Anderson, and L. W. Jaques. 1990. Preparation and purification of soybean lipoxygenase-derived unsaturated hydroperoxy and hydroxy fatty acids and determination of molar absorptivities of hydroxy fatty acids. *Anal. Biochem.* **188:** 38–47.
38. Bredeweg, R. A., L. D. Rothamn, and C. D. Pfieffer. 1979. Chemical reactivation of silica columns. *Anal. Chem.* **51:** 2061–2063.
39. Kuhn, H., R. Wiesner, V. Z. Lankin, A. Nekrasov, L. Alder, and T. Schewe. 1987. Analysis of the stereochemistry of lipoxygenase-derived hydroxypolyenoic fatty acids by means of chiral phase high-pressure liquid chromatography. *Anal. Biochem.* **160:** 24–34.
40. O'Flaherty, J. T., J. F. Cordes, S. L. Lee, M. Samuel, and M. J. Thomas. 1994. Chemical and biological characterization of oxo-eicosatetraenoic acids. *Biochim. Biophys. Acta.* **1201:** 505–515.
41. Oliw, E. H. 1989. Biosynthesis of 18(RD)-hydroxyeicosatetraenoic

acid from arachidonic acid by microsomes of monkey seminal vesicles. Some properties of a novel fatty acid omega 3-hydroxylase and omega 3-epoxygenase. *J. Biol. Chem.* **264:** 17845–17853.
42. Hammarström, S., and M. Hamberg. 1973. Steric analysis of 3-, 4,3- and 2-hydroxy acids and various alkanols by gas-liquid chromatography. *Anal. Biochem.* **52:** 169–179.
43. Oliw, E. H., K. Stark, and J. Bylund. 2001. Oxidation of prostaglandin H(2) and prostaglandin H(2) analogues by human cytochromes P450: analysis of omega-side chain hydroxy metabolites and four stereoisomers of 5-hydroxyprostaglandin I(1) by mass spectrometry. *Biochem. Pharmacol.* **62:** 407–415.
44. MacMillan, D. K., and R. C. Murphy. 1995. Analysis of lipid hydroperoxides and long-chain conjugated keto acids by negative ion electrospray mass spectrometry. *Am. Soc. Mass. Spectrom.* **6:** 1190–1201.
45. Murphy, R. C., R. M. Barkley, K. Zemski Berry, J. Hankin, K. Harrison, C. Johnson, J. Krank, A. McAnoy, C. Uhlson, and S. Zarini. 2005. Electrospray ionization and tandem mass spectrometry of eicosanoids. *Anal. Biochem.* **346:** 1–42.
46. Oliw, E. H., C. Su, T. Skogström, and G. Benthin. 1998. Analysis of novel hydroperoxides and other metabolites of oleic, linoleic, and linolenic acids by liquid chromatography-mass spectrometry with ion trap MSn. *Lipids.* **33:** 843–852.
47. Oliw, E. H., U. Garscha, T. Nilsson, and M. Cristea. 2006. Payne rearrangement during analysis of epoxyalcohols of linoleic and alpha-linolenic acids by normal phase liquid chromatography with tandem mass spectrometry. *Anal. Biochem.* **354:** 111–126.
48. Bylund, J., J. Ericsson, and E. H. Oliw. 1998. Analysis of cytochrome P450 metabolites of arachidonic and linoleic acids by liquid chromatography-mass spectrometry with ion trap MS. *Anal. Biochem.* **265:** 55–68.
49. Weber, H., B. A. Vick, and E. E. Farmer. 1997. Dinor-oxo-phytodienoic acid: a new hexadecanoid signal in the jasmonate family. *Proc. Natl. Acad. Sci. USA.* **94:** 10473–10478.
50. Chan, D. W-S., G. Levett, and J. A. Matthew. 1979. The mechanism of the rearrangement of linoleate hydroperoxides. *Chem. Phys. Lipids.* **24:** 245–256.